



The Natural History of Bruch's Membrane Calcification in Pseudoxanthoma Elasticum

Sara Risseeuw, MD,¹ Redmer van Leeuwen, MD, PhD,¹ Saskia M. Imhof, MD, PhD,¹ Wilko Spiering, MD, PhD,² Jeannette Ossewaarde-van Norel, MD, PhD¹

Purpose: To describe the natural history of Bruch's membrane (BM) calcification in patients with pseudoxanthoma elasticum (PXE).

Design: Retrospective cohort study.

Participants: Both eyes of 120 PXE patients younger than 50 years, 78 of whom had follow-up imaging after more than 1 year.

Methods: All patients underwent multimodal imaging, including color fundus photography, near-infrared reflectance (NIR) imaging, and late phase indocyanine green angiography (ICGA). We determined the distance from the optic disc to the central and temporal border of peau d'orange on NIR, expressed in horizontal optic disc diameter (ODD). The length of the longest angioid streak was classified into 5 zones.

Main Outcome Measures: Age-specific changes of peau d'orange, angioid streaks, and ICGA hypofluorescence as surrogate markers for the extent of BM calcification.

Results: In cross-sectional analysis, longer angioid streaks were associated with increasing age ($P < 0.001$ for trend). The temporal border of peau d'orange showed a weak association with increasing age ($\beta = 0.02$; 95% confidence interval [CI], 0.00–0.04), whereas the central border showed a strong association ($\beta = 0.12$; 95% CI, 0.09–0.15). Longitudinal analysis revealed a median shift of the central border to the periphery of 0.08 ODD per year (interquartile range [IQR], 0.00–0.17; $P < 0.001$). This shift was more pronounced in patients younger than 20 years (0.12 ODD per year [IQR, 0.08–0.28]) than in patients older than 40 years (0.07 ODD per year [IQR, –0.05 to 0.15]). The temporal border did not shift during follow-up ($P = 0.69$). New or growing angioid streaks were detected in 39 of 156 eyes (25%). The hypofluorescent area on ICGA was visible only in the fourth or fifth decade and correlated with longer angioid streaks.

Conclusions: In PXE patients, the speckled BM calcification slowly confluent during life. The location of the temporal border of peau d'orange remains rather constant, whereas the central border shifts to the periphery. This suggests the presence of a predetermined area for BM calcification. A larger ICGA hypofluorescent area correlates with older age and longer angioid streaks, which implies that it depends on the degree of BM calcification. *Ophthalmology Science* 2021;1:100001 © 2021 by the American Academy of Ophthalmology. This is an open access article under the CC BY-NC-ND license (<http://creativecommons.org/licenses/by-nc-nd/4.0/>).

Pseudoxanthoma elasticum (PXE) is a rare autosomal recessive disorder (Online Mendelian Inheritance in Man identifier, 264800) in which a biallelic mutation in the *ABCC6* gene leads to calcification of elastic fibers in the skin, vasculature, and Bruch's membrane (BM) of the eyes.^{1–3} Bruch's membrane calcification eventually causes macular degeneration and subsequent visual impairment at a relatively young age.^{4–7}

The typical manifestations of BM calcification in the fundus are peau d'orange and angioid streaks.^{8,9} Peau d'orange describes the speckled pattern seen with funduscopy and near-infrared reflectance (NIR) imaging and is believed to be the transition zone between a calcified BM and a normal fundus.^{10,11} The presence of peau d'orange precedes the formation of angioid streaks in the brittle calcified BM.^{12,13} Angioid streaks are breaks in BM that are visible as irregular jagged lines in the fundus and probably are caused by mechanical stress exerted on the eye.¹⁴ Angioid streaks are not visible yet at birth and are

believed to occur around the second decade of life.¹³ In younger patients, peau d'orange often is present in the posterior pole, whereas, in later disease stages, more peripheral peau d'orange often appears.⁷ Furthermore, on late-phase indocyanine green angiography (ICGA), a typical hypofluorescent area with a speckled border is found in the posterior pole, mimicking peau d'orange, but located more centrally.¹⁰ These findings led to the hypothetical model of a centrifugal spread of BM calcification by Charbel Issa et al.¹⁰

Little information is available on the natural course of BM calcification. The recent start of therapeutic developments, such as etidronate and dietary pyrophosphate, necessitates knowledge on the natural course of BM calcification.^{15,16} Also, a larger extent of BM calcification increases the risk for macular degeneration in PXE patients and thereby has an impact on visual prognosis.¹⁷ However, before resulting in central visual loss, BM calcification in PXE has an insidious effect on the

structure and function of different cell types in the retina, the retinal pigment epithelium (RPE), and the choroid that presents as choroidal thinning and on certain aspects of visual function, such as a reduced dark adaptation in young patients.^{18–21}

We aimed to investigate the natural history of BM calcification in PXE patients younger than 50 years, before the onset of frequent macular degeneration in the sixth decade that impedes the assessment of early clinical features in the fundus of a PXE patient. We studied the age-specific manifestations of peau d'orange, angioid streaks, and ICGA hypofluorescence, which we used as surrogate or indirect markers for BM calcification. Moreover, we studied longitudinal changes of these features over at least 1 year.

Methods

Design and Study Population

We performed this retrospective cross-sectional, longitudinal cohort study within the Dutch National Expertise Center for PXE, a multidisciplinary tertiary referral center that is situated at the University Medical Center Utrecht, Utrecht, The Netherlands. We included all patients who had a clinical diagnosis of PXE according to the criteria proposed by Plomp et al,² which was confirmed with either a biallelic *ABCC6* mutation or skin biopsy. All research adhered to the tenets of the Declaration of Helsinki. The institutional ethics committee approved the study protocol (identifier, METC 19/257), and additional written informed consent was obtained from all patients who agreed to undergo a late-phase ICGA (identifier, METC 18/767). We included patients younger than 50 years at the time of the first 55° NIR imaging of the retina. This resulted in a study population of 120 patients.

Ophthalmologic Data

The standard ophthalmologic examination included best-corrected-visual acuity (BCVA) measurement and funduscopy. Retinal imaging consisted of color fundus photography (FF 450 plus; Carl Zeiss Meditec AG), spectral-domain (SD) OCT, 55° NIR imaging, and fundus autofluorescence (FAF; all 3 by Spectralis HRA-OCT [Heidelberg Engineering]). Late-phase ICGA was performed either for clinical indication or for research purposes with the patient's approval and written informed consent. If the patient had visited our department more than once, we also investigated the data on the most recent visit. We classified the BCVA of the better eye according to the severity of visual impairment using the criteria of the World Health Organization.²²

Assessment of Angioid Streaks

We measured the spread of angioid streaks as a proxy for the extent of BM calcification.^{10,17} Using 55° NIR imaging, we evaluated the length of the longest angioid streak from the center of the optic disc by comparing its length with 3 circles centered on the center of the optic disc with respective radii of 3 mm, 6 mm, and 9 mm using the Heidelberg Eye Explorer software (Heidelberg Engineering). This was graded into angioid streaks extending less than 3 mm from the center of the optic disc (zone 1), those extending 3 to 6 mm from the center of the optic disc (zone 2), those extending 6 to 9 mm from the center of the optic disc (zone 3), and those extending more than 9 mm from the center of the optic disc (zone 4). Some eyes with peau d'orange did not have detectable angioid streaks. The grading of angioid streaks was without regard for their topographical location in the retina and was based on both central and mid-peripheral 55° NIR imaging.

Also, we graded the presence of angioid streaks in the macula by manually positioning the Early Treatment Diabetic Retinopathy Study grid on the foveal dip and grading the presence or absence of angioid streaks in the central 3000- μ m diameter on 30° NIR imaging. Furthermore, we assessed longitudinal changes

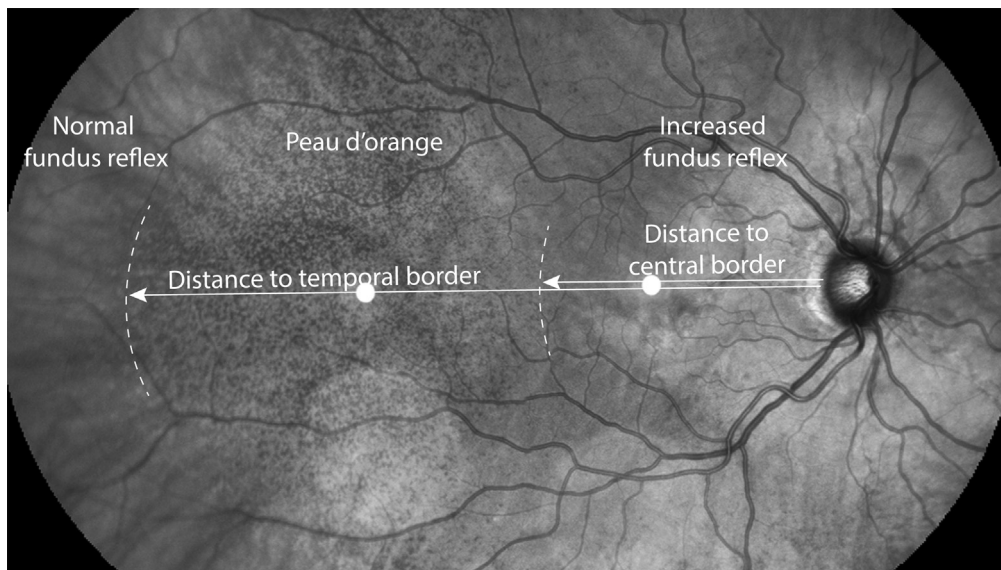


Figure 1. Assessment of the borders of peau d'orange in patients with pseudoxanthoma elasticum using near-infrared reflectance (NIR) imaging. The 55° central and temporal NIR images were merged. The temporal and central border of peau d'orange were defined as ending at an area with characteristic speckling with hyporeflectivity and hyperreflectivity on NIR imaging along a line through the optic disc and the fovea. The white dots on the papillofoveal axis are imaging artefacts.

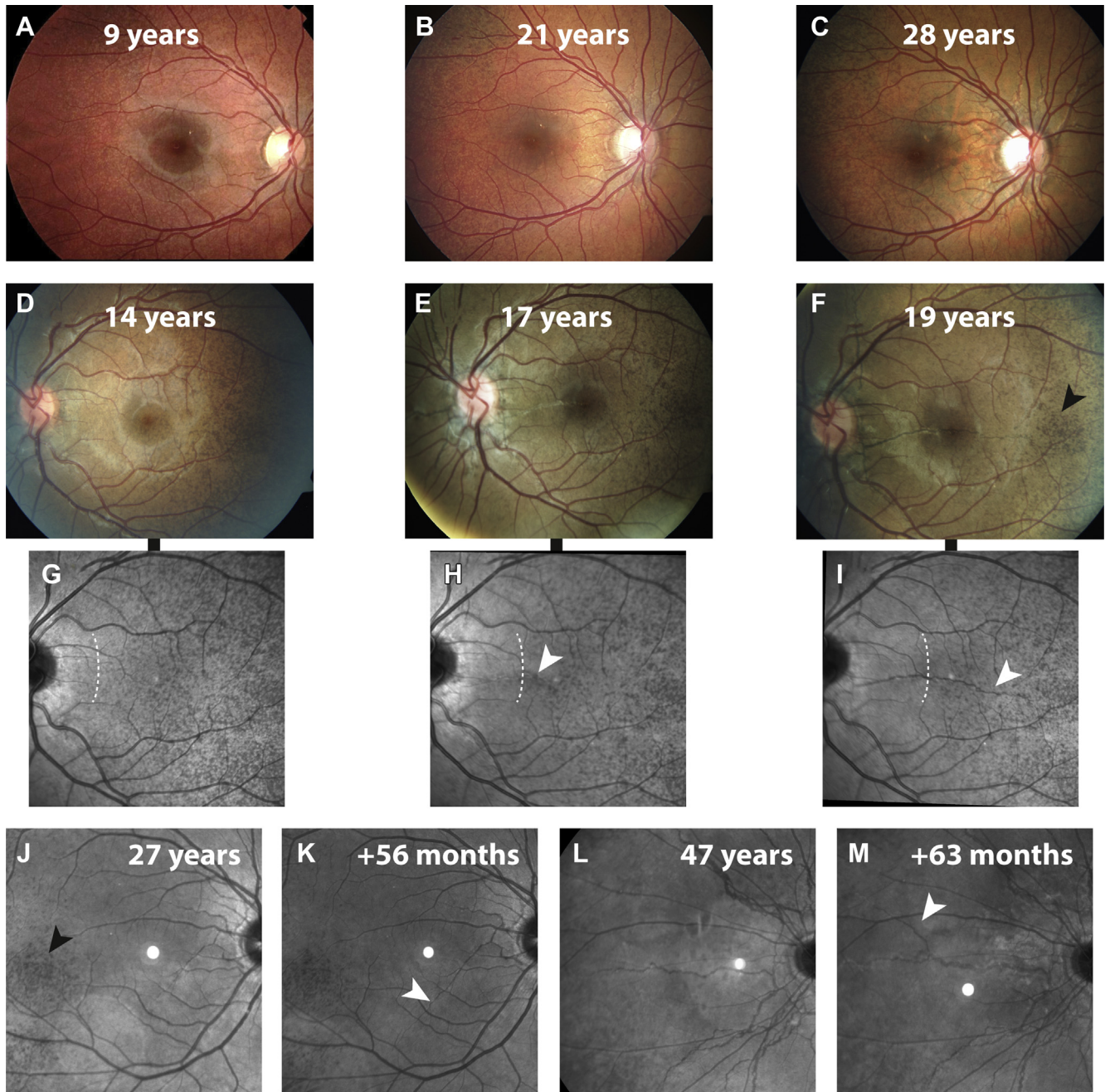


Figure 2. Progression of angioid streaks and peau d'orange in patients with pseudoxanthoma elasticum (PXE). A–C, Fundus photographs of the right eye of a female patient at (A) 9, (B) 21, and (C) 28 years of age. The first fundus photograph (A) reveals only peau d'orange, which progressed together with the (B) appearance and (C) growth of angioid streaks. D–I, Fundus photographs (D–F) and corresponding 30° near-infrared reflectance (NIR) imaging (G–I) from a female patient at 14 years of age with follow-up imaging after 37 months (at 17 years of age) and 56 months (at 19 years of age). The white arrowheads indicate the development of a new angioid streak in the macula (H), which grows further in less than 2 years (I). Progression of the central border of peau d'orange is visible on 30° NIR imaging and is indicated with dashed lines (G, I). J–M, Growth of or appearance of new angioid streaks were assessed with 55° NIR imaging in two patients. J, K, Lengthening of an angioid streak (K) with a follow-up interval of 56 months after the first visit at 27 years of age (J). L, M, Occurrence of new angioid streaks presenting as a new branch nasal of the optic nerve visible in a patient 47 years of age (L) at baseline with (M) an interval of 63 months. The black arrowheads in (F, J) indicate islands of decreased reflectivity in NIR imaging, so-called temporal sparing.

of angioid streaks. To do so, we compared all available central and mid-peripheral 55° NIR imaging of the first and last visit to determine lengthening of or new angioid streaks, branching angioid streaks, or both new and branching angioid streaks. Last,

we assessed changes in angioid streaks within the central 3000 μm by comparing the first and last 30° NIR imaging. If necessary, fundus photography was used to verify changes in angioid streaks.

Table 1. Patient Characteristics

Characteristic	Overall (n = 120)	Age Group (yrs)				Nominal P Value	P Value for Trend*
		0–19 (n = 17)	20–29 (n = 26)	30–39 (n = 23)	40–49 (n = 54)		
Female gender	86 (72)	13 (77)	22 (85)	19 (83)	32 (59)	0.05	0.04
Phenotype [†]							
BCVA (decimal)							
Best eye	1.15 (1.00–1.23)	1.05 (1.00–1.20)	1.20 (1.07–1.41)	1.20 (1.00–1.35)	1.05 (0.95–1.20)	0.14	0.13
Worst eye	0.98 (0.80–1.10)	0.95 (0.83–1.00)	1.05 (0.95–1.20)	1.00 (0.85–1.15)	0.89 (0.63–1.00)	0.003	0.009
Presence of (in) active CNV	15 (13)	0	0	1 (4)	14 (26)	0.001	0.02
Macular atrophy	3 (3)	0	0	0	3 (6)	0.28	>0.99
Pattern dystrophy- like changes	13 (9)	0	0	0	13 (21)	0.002	0.99
Angioid streaks [‡]							
Extent from optic disc (mm)							
0	7 (6)	7 (41)	0	0	0	<0.001	<0.001
<3	3 (3)	0	2 (8)	0	1 (2)		
3–6	45 (38)	7 (41)	14 (54)	11 (48)	13 (24)		
6–9	26 (22)	2 (12)	6 (23)	6 (26)	12 (22)		
>9	39 (33)	1 (6)	4 (15)	6 (26)	28 (52)		
In central 3000 μm Peau d'orange (ODD) [§]	66 (56)	5 (29)	9 (35)	14 (61)	38 (72)	0.002	<0.001
Temporal border	8.7 (7.8–9.8)	8.5 (7.9–9.4)	8.6 (7.8–9.2)	8.6 (7.7–9.7)	8.7 (8.1–10.2)	0.53	0.04
Central border	2.6 (1.5–4.9)	1.2 (0.9–1.5)	1.8 (1.4–2.5)	3.7 (1.6–4.9)	4.7 (3.0–7.1)	<0.001	<0.001

BCVA = best-corrected visual acuity; CNV = choroidal neovascularization; ODD = horizontal optic disc diameter.

Data are presented as no. (%) or median (interquartile range). Nominal testing for difference is based on the chi-square test and Mann–Whitney *U* test.

*The *P* value for trend was the *P* value of the estimate of the age category as a continuous determinant in a linear, logistic, or ordinal regression analysis, with the corresponding patient characteristic as outcome.

[†]Details are presented for right eyes.

[‡]The temporal border in the right eye could be measured in 111 eyes and the central border could be measured in 114 eyes.

Assessment of Peau d'Orange

We measured the distance of the central and peripheral borders of peau d'orange on NIR imaging along a virtual axis from the temporal border of the optic disc to the temporal periphery through the fovea (Fig 1). For each eye, we assembled the central and the temporal 55° NIR imaging to create an aligned montage (Adobe Photoshop CS6; Adobe Systems, Inc). The peripheral and central borders of peau d'orange were defined as the temporal and central ending of an area with characteristic speckling with hyporeflectivity and hyperreflectivity on NIR, respectively. We used color fundus photography and 30° NIR imaging to verify the location of the borders, if necessary.

In some patients, the central border of the peau d'orange coincided with temporal sparing, a phenomenon of an island of relative decreased reflectivity temporal from the macula (Fig 2F, J).¹⁰ Most PXE patients demonstrate temporal sparing, and we assume that it is a phenomenon that is independent of the spread of BM calcification. However, the speckled aspect of temporal sparing resembles peau d'orange, which impedes the assessment of peau d'orange if it is the central border in that area. Therefore, if the temporal sparing coincided with the presumed central border of peau d'orange, we assessed the total area of peau d'orange within the posterior pole to determine a virtual vertical axis that defines the central border of peau d'orange. Then, the crossing of this axis with the virtual axis through the fovea was defined as the position of the central border.

Measurements were made semiquantitatively by using the horizontal optic disc diameter (ODD) as the measurement unit in ImageJ (ImageJ; National Institutes of Health). The ODD was chosen to enable longitudinal measurements within 1 patient and to correct for differences in refraction error and image settings.

We assessed the intraobserver and interobserver reproducibility of this measurement in a subset of 10 patients (20 eyes). For the temporal border, the intraobserver agreement showed a mean difference of -0.13 ODD (95% limits of agreement, -0.80 to 0.55). The intraobserver reliability was excellent, with an intraclass correlation coefficient (ICC) of 0.96 (95% confidence interval [CI], 0.89 – 0.98).²³ The central border showed an intraobserver difference of -0.02 (95% limits of agreement, -0.51 to 0.46) and also high reliability (ICC, 0.99 ; 95% CI, 0.99 – 1).

Interobserver reproducibility was assessed by 3 graders (S.R., R.v.L., J.O.v.N.) and analyzed in 3 pairs of measurements. For the temporal border, the mean differences were -0.25 , 0.01 , and 0.08 ODD, and the ICCs were moderate to excellent (0.69 , 0.87 , and 0.83 , respectively).²³ For the central border, the mean differences were 0.07 , 0.25 , and 0.28 ODD, and the ICCs were moderate to excellent (0.86 , 0.95 , and 0.64 , respectively).²³

Ophthalmologic Phenotype

We graded the presence of (in)active choroidal neovascularization (CNV) and macular atrophy in the posterior pole per eye. A CNV was present in case of subretinal or intraretinal fluid; a neovascular

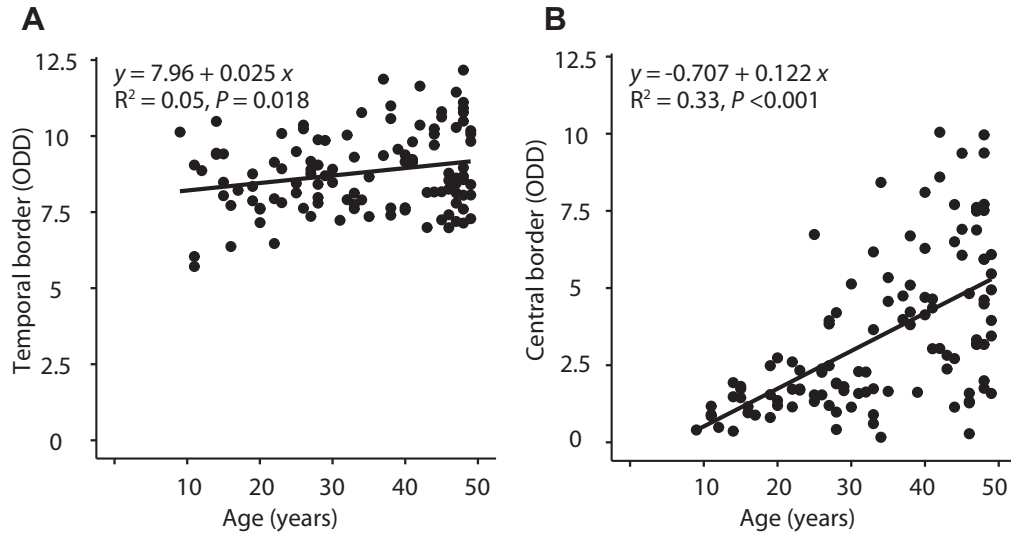


Figure 3. Scatterplots showing the correlation between age and extent of peau d'orange: (A) temporal and (B) central border of the peau d'orange in optic disc diameter (ODD). Data are presented for the right eye only. The temporal border could be measured in 111 eyes, and the central border could be measured in 114 eyes. In the top left of (A), the regression equation (with age as determinant and distance as dependent variable) is displayed, with less than the R^2 value and the P value for the estimate.

complex on SD OCT; leakage of CNV; staining of scars on fluorescein angiography or ICGA; hemorrhage, scarring, or hyperpigmentation on color fundus photography; or a combination thereof. Grading of macular atrophy was based on the loss of the RPE signal on SD OCT, sharply demarcated areas of hypofluorescence on FAF and hypopigmentation and visible choroidal vessels on color fundus photography in the posterior pole with a minimal size of the atrophic largest lesion of at least half the area of the optic disc.

The presence of pattern dystrophy-like changes was graded on FAF imaging and was defined as focally increased autofluorescence in the posterior pole resembling pattern dystrophies in an area of at least 1 ODD diameter.^{24,25} If available, the late-phase ICGA imaging was assessed for the presence of a speckled hypofluorescent area superimposed on the physiologic

hypofluorescence in the macula.¹⁰ Late-phase ICGA was captured at least 30 minutes after administration of the indocyanine green dye.

Data Analyses

Categorical data are presented as numbers (percentages), normally distributed data are presented as mean±standard deviation, and data with a nonparametric distribution are presented as median (interquartile range [IQR]). Differences between groups were tested with the Pearson chi-square test or the Mann–Whitney U test when appropriate. The 1-sample Wilcoxon signed-rank test was used to test for a longitudinal difference of the border of peau d'orange. To test for a trend effect of age on baseline

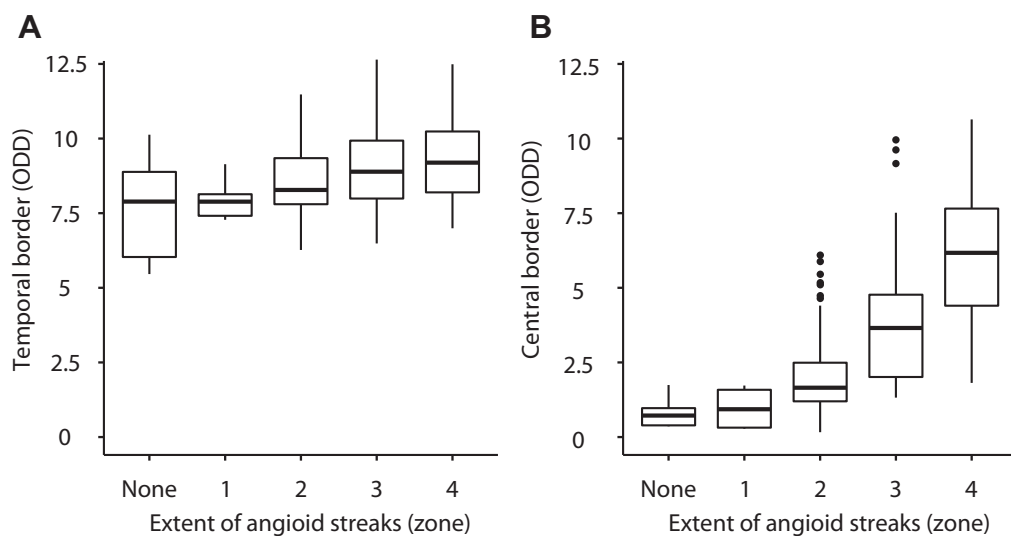


Figure 4. Box-and-whisker plots showing the correlation between extent of angioid streaks and extent of peau d'orange: median and interquartile range of the extent of peau d'orange, expressed as optic disc diameter (ODD), for the (A) temporal border and (B) central border, stratified for the extent of angioid streaks. Data are presented per eye.

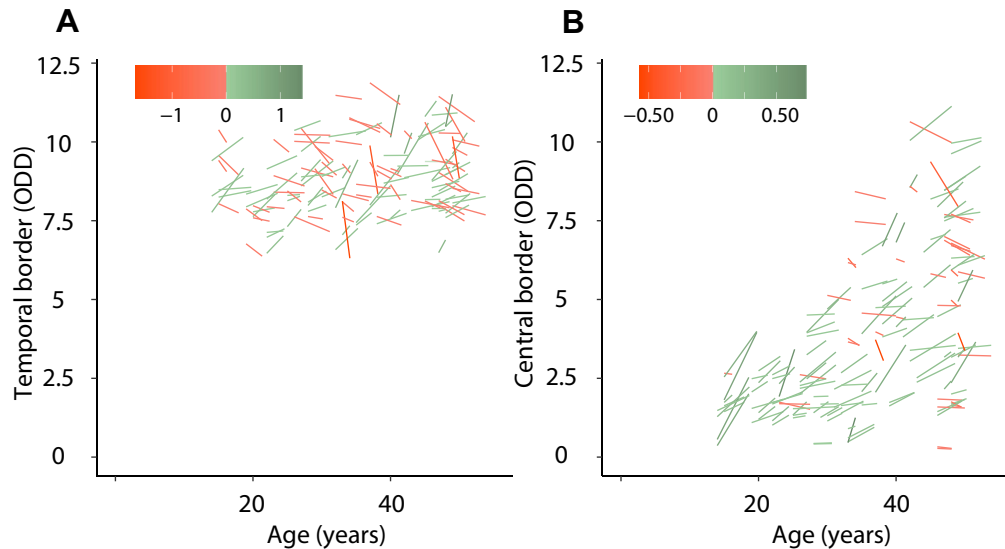


Figure 5. Graphs showing repeated measures of the (A) temporal and (B) central border of peau d'orange for patients with a minimum follow-up of 12 months. Each line represents 1 patient. The x-axis represents the age of the patient and the y-axis represents the eccentricity of the peau d'orange in optic disc diameter (ODD) per eye. The color of the lines represent the magnitude of the change (between baseline and follow-up) in ODD per year.

characteristics, logistic or linear regression models were built with the age group as a determinant and the baseline characteristic as an outcome variable. To investigate longitudinal changes, we excluded patients with a follow-up duration of less than 12 months. To obtain information on the progression of peau d'orange, we calculated the difference of the borders of peau d'orange between the first and last visit. Then, we corrected this for the duration of follow-up to obtain a measure of change per 1 year of follow-up.

Associations between age and peau d'orange and angioid streaks were investigated with linear regression analysis with the right eye as the outcome. Linear mixed-model analysis was used to test for differences on eye level while correcting for both eyes of a patient and to test for a trend effect of angioid streaks on peau d'orange on eye level. The dependent variable was set as a fixed effect, and the individual patient was modeled as a random intercept. A *P* value of less than 0.05 was considered statistically significant. We used R software version 3.6.1 (R Foundation for Statistical Computing) for data analysis. The package nlme (version 3.1-140) was used for mixed-model analysis.

Results

In total, 120 PXE patients were included, all having peau d'orange of the retina or 1 or more angioid streaks, each at least as long as 1 ODD.² Bi-allelic *ABCC6* mutations were found in 116 patients. In 1 patient, only 1 mutation was found; in 2 patients, no mutations were found; and 1 patient did not undergo genetic testing. The latter 4 patients all underwent skin biopsy examination that confirmed the PXE diagnosis. The median age was 37 years (IQR, 26–46 years), ranging from 9 to 49 years, and 86 of them (72%) were women. Further characteristics of the total group and stratified per decade of age are presented in Table 1. Two patients, both in the fifth decade of life, were visually impaired because of PXE-related macular degeneration and 2 patients had an amblyopic eye.

Angioid Streaks

Cross-sectional Analysis. The length of angioid streaks was associated with age (Table 1). The percentage of patients with the longest angioid streaks increased from 6% in patients 0 to 19 years of age to 52% in patients 40 to 49 years of age. The mean age of the 7 patients without angioid streaks was 12 ± 2 years. For zone 1 ($n = 3$), the mean age was 31 ± 13 years; for zone 2 ($n = 45$), the mean age was 32 ± 11 years; for zone 3 ($n = 26$), the mean age was 37 ± 11 years; and for zone 4 ($n = 39$), the mean age was 41 ± 8 years. Angioid streaks in the central $3000 \mu\text{m}$ of the macula were present in 130 eyes of 76 PXE patients (54% of all eyes). In 3 eyes of 2 patients, the presence of macular angioid streaks could not be assessed because of extensive pathologic features.

Longitudinal Analysis. Of all patients, 78 underwent follow-up imaging with a minimum duration of 1 year (median duration, 41 months; IQR, 26–53 months). The imaging of these patients was evaluated for changes in length and development of new angioid streaks. Of the 156 eyes, 117 (75%) did not show changes in angioid streaks. However, in 27 eyes (17%) of 23 patients (mean age at baseline, 30 years; range, 15–48 years), we observed lengthening of angioid streaks. In 12 eyes (8%) of 11 patients (mean age at baseline, 31 years; range, 14–48 years), we observed new (branches of) angioid streaks. In total, changes in angioid streaks were observed in 39 eyes (25%) with a cumulative follow-up of 254 patient years. Examples of patients with changes in angioid streaks are presented in Figure 2. New angioid streaks in the central $3000 \mu\text{m}$ of the macula developed in 5 eyes of 4 patients. These new streaks developed at 16 years of age (in both eyes), 28 years of age, 44 years of age, and 48 years of age. In total, longer or new angioid streaks in the central $3000 \mu\text{m}$ of the macula were

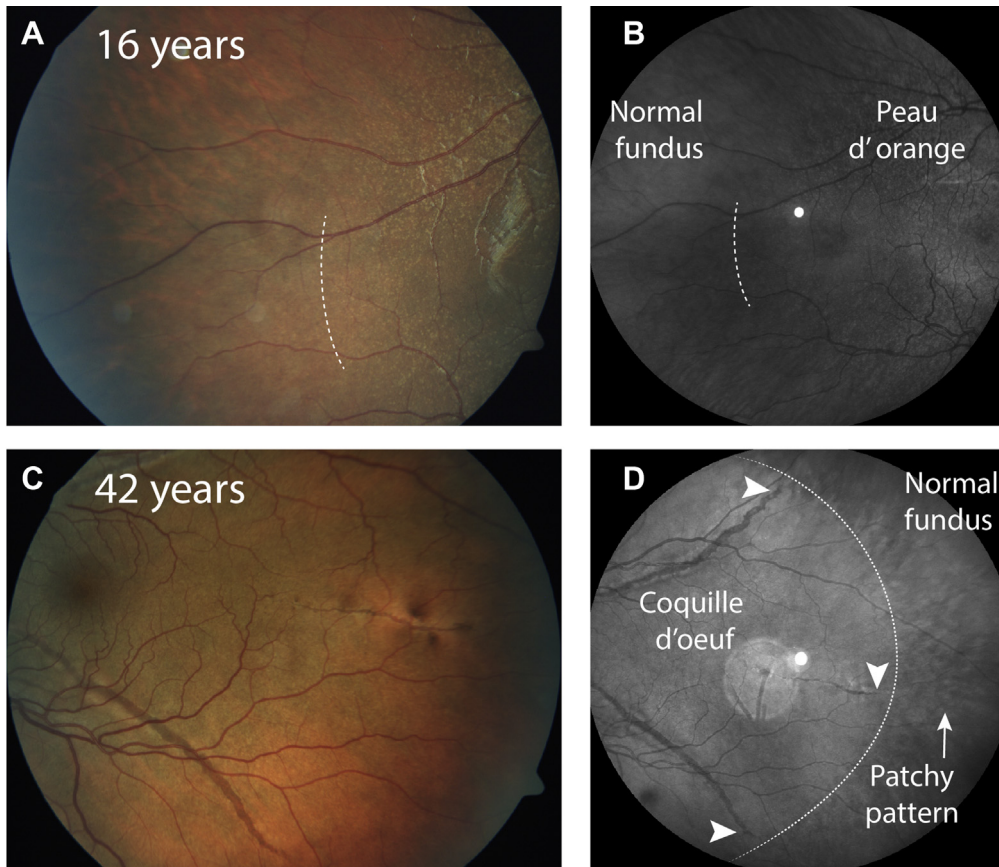


Figure 6. Characteristics of the temporal border of peau d'orange of 2 patients. One patient is in (A, B) an early stage of the disease stage, and the other is in (C, D) a late stage of the disease. A, B, No angioid streaks are visible yet, and the temporal peau d'orange shows a sparsely speckled pattern that is best visible on color fundus photography. The border is indicated with a dashed line. C, D, In contrast, Bruch's membrane calcification appears confluent and angioid streaks extend to the periphery. No typical peau d'orange is visible. D, The angioid streaks extend to the far periphery in the coquille d'oeuf (white arrowheads), and a patchy pattern is visible peripheral from the coquille d'oeuf. The dotted line indicates the approximate border between the coquille d'oeuf and the limited peau d'orange.

observed in 10 eyes (6%) with a cumulative follow-up of 254 patient years.

Peau d'Orange

Cross-sectional Analysis. The temporal border of peau d'orange could be measured in 221 eyes of 116 PXE patients, and the central border could be measured in 229 eyes of 117 PXE patients. The location of the temporal border remained rather constant with increasing age, whereas the location of the central border shifted to the temporal periphery with age (Table 1). The temporal border ranged from 8.5 ODD in patients 0 to 19 years of age to 8.7 ODD in patients 40 to 49 years of age. A small but statistically significant association was found between temporal border and age ($\beta = 0.02$ ODD; 95% CI, 0.00–0.04; Fig 3). The central border ranged from 1.2 ODD in patients 0 to 19 years of age to 4.7 ODD in patients 40 to 49 years of age. The association with age was much stronger for the central border ($\beta = 0.12$ ODD; 95% CI, 0.09–0.15). The length of the longest angioid streak was associated with both the location of the temporal border ($\beta = 0.38$ ODD;

95% CI, 0.20–0.57; Fig 4) and even more strongly with the location of the central border ($\beta = 0.67$ ODD; 95% CI, 0.45–0.89) of the peau d'orange.

Longitudinal Analysis. In the 78 patients (156 eyes) with at least 1 year follow-up, 72 of the 140 eyes (51%) with repeated measurements of the temporal border showed a positive shift and 68 eyes (49%) showed a negative shift (a positive shift was defined as a temporal shift and a negative shift was defined as a nasal shift). For the central border, 150 eyes showed repeated measurements, of which 112 (75%) showed a positive shift and 38 eyes (25%) showed a negative shift. The repeated measurements per eye are visualized in relation to patient age in Figure 5.

The temporal border of peau d'orange did not progress within a patient (median, 0.00 ODD per year; IQR, –0.12 to 0.12 ODD per year; $P = 0.69$). The central border did progress with a statistically significant median shift to the temporal periphery of 0.08 ODD per year (IQR, 0.00–0.17 ODD per year; $P < 0.001$). This shift was larger in younger patients: the median progression in patients younger than 20 years at baseline was 0.12 ODD per year (IQR, 0.08–0.28 ODD per

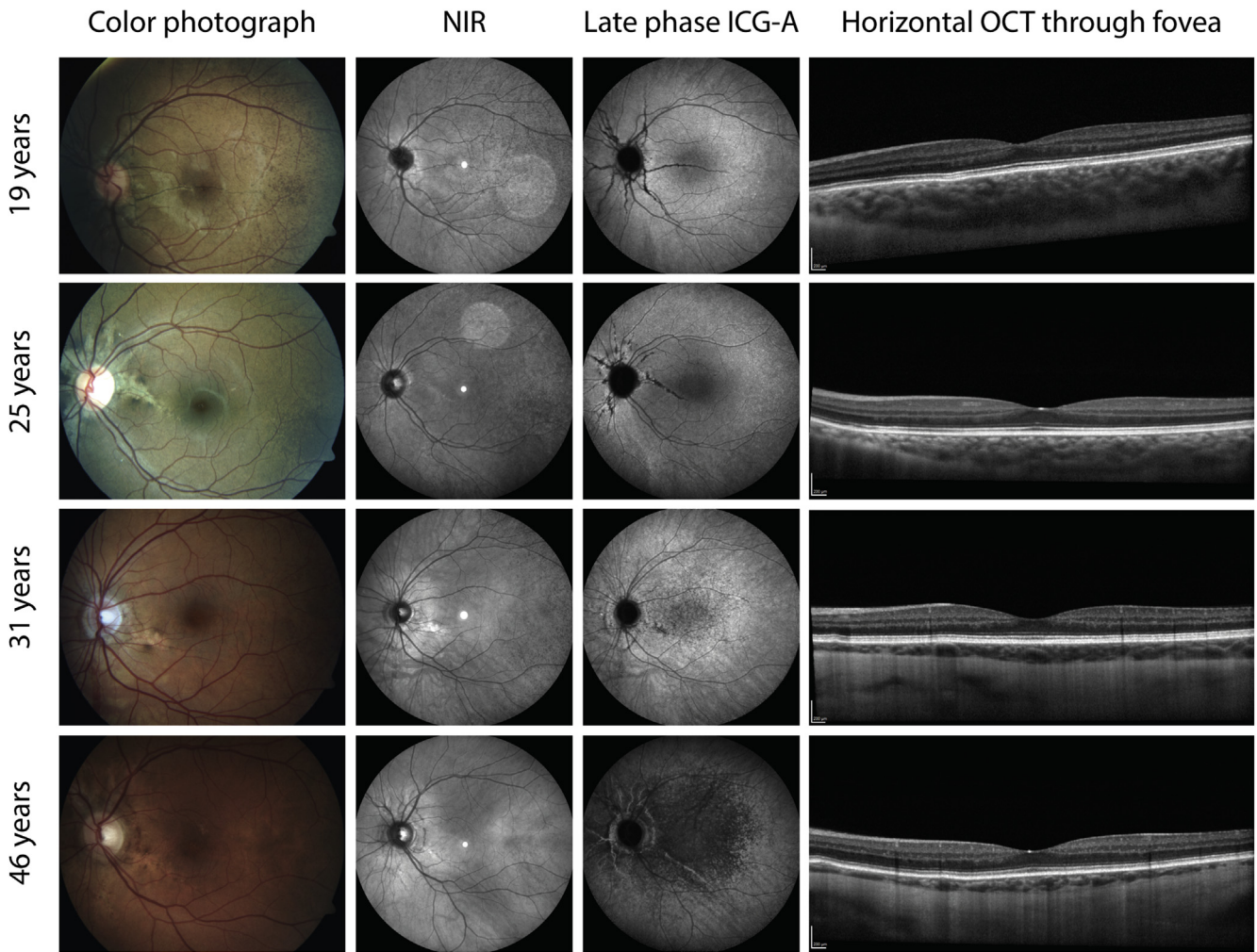


Figure 7. Typical multimodal imaging of 4 pseudoxanthoma elasticum patients in different decades, all without choroidal neovascularization or atrophy. The first column shows color fundus photographs, the second column shows near-infrared reflectance (NIR) imaging, the third column shows late-phase indocyanine green angiography (ICGA), and the fourth column shows horizontal OCT imaging through the fovea. In the younger patients, no pattern of hypofluorescence appears on late-phase ICGA yet. After 30 years of age, a central area of hypofluorescence appears (third row), which often progresses until the fifth decade (bottom row). This pattern of hypofluorescence on ICGA does not seem to correlate with findings on color photographs, NIR imaging, or OCT.

year), that in patients 20 to 29 years of age was 0.09 ODD per year (IQR, 0.01–0.18 ODD per year), that in patients 30 to 39 years of age was 0.09 ODD per year (IQR, –0.01 to 0.14 ODD per year), and that in patients 40 to 49 years of age was 0.07 ODD per year (IQR, –0.05 to 0.15 ODD per year). Examples of patients with progression of the central border of peau d’orange are presented in [Figure 2](#).

The appearance of the temporal border differed between young and older patients. In younger patients, for example, those younger than 20 years, the temporal border appeared sparsely speckled (patient 1 in [Fig 6](#)). Some older patients with nearly confluent BM calcification showed a patchy pattern around the confluent BM calcification (patient 2 in [Fig 6](#)).

Late-Phase Indocyanine Green Angiography

Twenty-three PXE patients underwent late-phase ICGA. Of those patients, 1 was younger than 20 years, 3 were 20 to 29

years of age, 4 were 30 to 39 years of age, and 15 were older than 40 years. The PXE-specific changes of a hypofluorescent area and a speckled transition zone were symmetrical over both eyes.

The 16 patients with a hypofluorescent area or speckles (median age, 44 years; IQR, 42–48 years) were older than the 7 patients without a hypofluorescent area or speckles (median age, 28 years; IQR, 23–36 years; $P = 0.002$). The youngest patient with hypofluorescent speckles was 31 years, and the oldest patient without hypofluorescent speckles was 45 years. Age-specific examples of multimodal imaging, including ICGA, are presented in [Figure 7](#). Early hypofluorescent changes were visible in the macular area and showed subtle, but detectable, centrifugal progression over time ([Fig 8](#)). Temporal sparing, defined as an island of normal fluorescence in the hypofluorescent area on ICGA, seemed to disappear over time by becoming confluent hypofluorescent ([Fig 8](#), A, C, D, F).

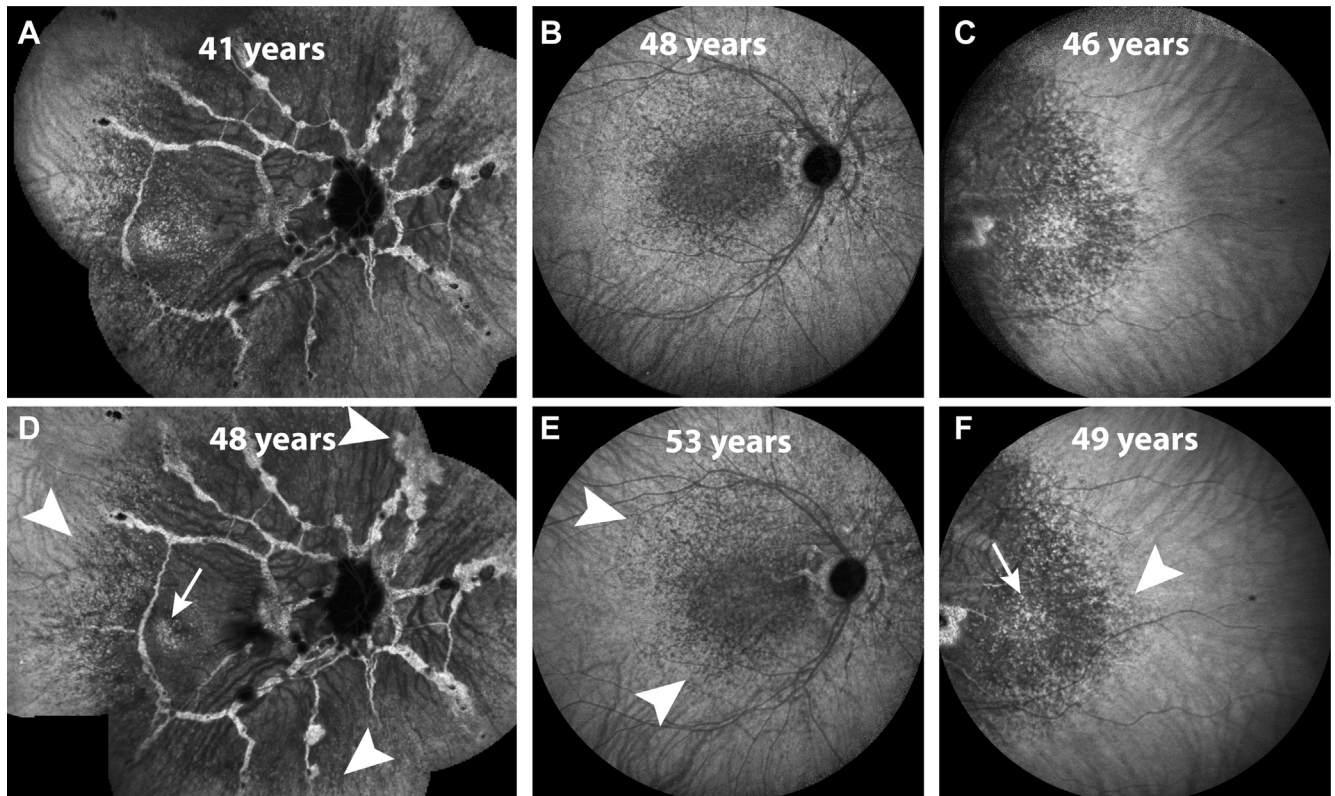


Figure 8. Late-phase indocyanine green angiography images of 3 patients with follow-up imaging in the rows below: fundus photographs of a right eye at (A) 41 years and (D) 48 years of age; posterior pole of a right eye at (B) 48 years and (E) 53 years of age; and temporal imaging of a left eye at (C) 46 years and (F) 49 years of age. The hypofluorescent speckled central area is characteristic of pseudoxanthoma elasticum patients. The mostly subtle changes are indicated by white arrowheads. The white arrows indicate the temporal island that seems to disappear over time by becoming confluent hypofluorescent.

The extent of the hypofluorescent area on ICGA imaging varied largely between patients of similar age, which seemed to correlate with the length of angioid streaks. The longer the angioid streaks, the larger the ICGA hypofluorescent area. This is illustrated in [Figure 9](#).

Discussion

This study provides detailed information on the spread of peau d'orange in a large cohort of relatively young PXE patients. The central border likely demarcates confluent BM calcification and progresses in both cross-sectional and longitudinal analyses. The peripheral border demarcates the normal fundus appearance and shows very little progression toward the retinal periphery ([Fig 3](#)). This suggests that the area of confluent BM calcification enlarges, in contrast to the area of peau d'orange, or the second transition zone,¹⁰ which does not spread centrifugally, but rather becomes narrower. This is supported by the finding that in some younger patients, the peripheral speckled borders are hardly detectable and become more pronounced with increasing age ([Fig 6](#)).

Based on these findings, we hypothesize that a pre-determined area exists for BM calcification that is visible early in life as peau d'orange throughout the posterior pole.

With age, the BM calcification progresses and conflues, which leads to an area of confluent BM calcification with an increased fundus reflex. The larger this area of confluent BM calcification is, the narrower the zone of peau d'orange will become and the more peripherally it will be visible. Later in life, in the fourth or fifth decade, a hypofluorescent pattern will appear on late-phase ICGA. This area starts in the macula and then spreads centrifugally. This hypothesis is a modification of the model proposed by Charbel Issa et al,¹⁰ and a modified schematic figure is presented in [Figure 10](#).

The application of the border of peau d'orange as a surrogate marker for the extent of BM calcification in PXE is not a new concept. Two studies measured the central border of peau d'orange and found an association with more reticular pseudodrusen and with reduced quantitative autofluorescence.^{26,27} These measurements were performed on 30° macular NIR imaging, but in most eyes with PXE, the peau d'orange extends further to the periphery than 30° or 8.6 mm from the temporal border of the optic disc. We adjusted the aforementioned method to a standardized semiquantitative measurement that is suitable for both central and peripheral measurements.

The strong correlation of the central border of peau d'orange with the extent of angioid streaks confirms our interpretation of the central border as a surrogate marker

Length of angioid streaks

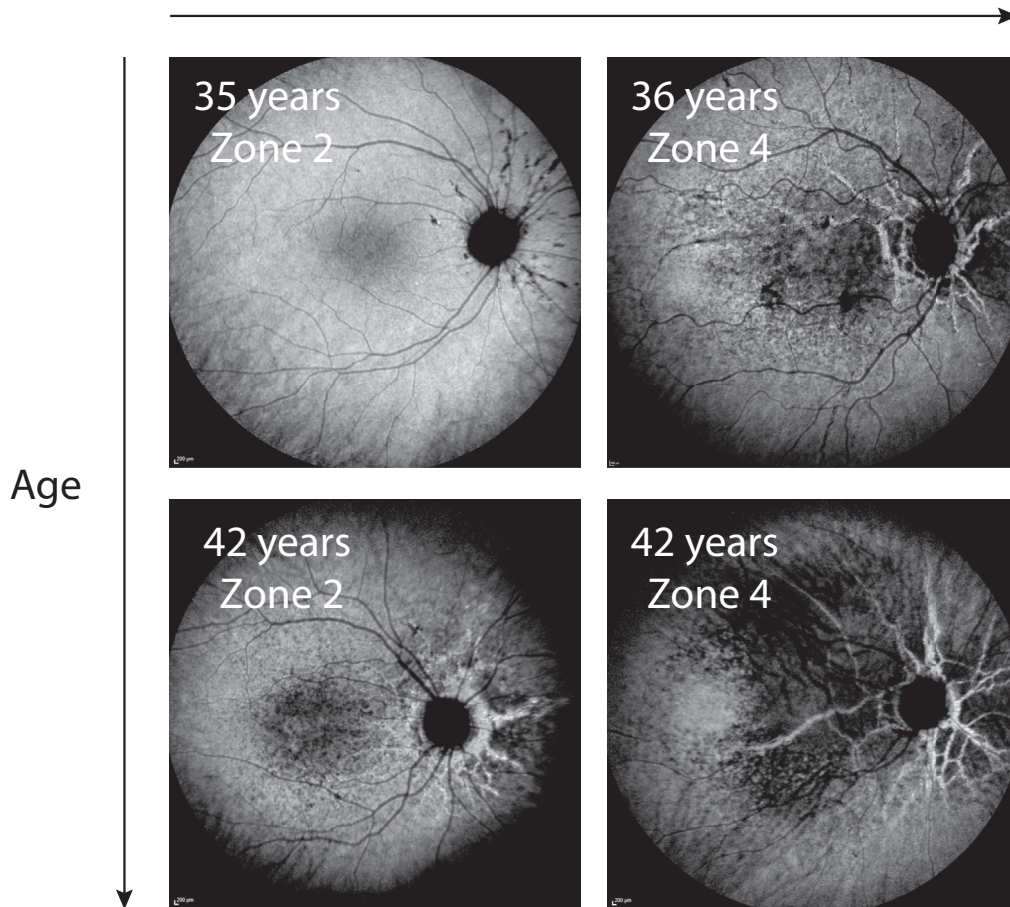


Figure 9. Characteristics of late-phase indocyanine green (ICG) hypofluorescence in 4 different pseudoxanthoma elasticum patients with comparable ages, but different lengths of angioid streaks. In zone 2, the longest angioid streak extends 3 to 6 mm from the center of the optic disc, whereas in zone 4, the longest angioid streaks extend more than 9 mm from the center of the optic disc. Longer angioid streaks seem to correlate with more extensive ICG hypofluorescence.

for the extent of BM calcification. However, this method relies on a subjective assessment of the border. The intragrader reproducibility was excellent, but the intergrader reproducibility showed more variation, partly because of different assessments of the ODD. Therefore, we emphasize that this method allows for cross-sectional and longitudinal comparisons within a cohort, but comparisons of absolute values between cohorts should be interpreted with caution.

We observed that the hypofluorescent area on late-phase ICGA is larger in older patients if compared with younger patients and that slow progression can be detected over a timespan of several years. Furthermore, the hypofluorescence seems to correlate with the length of the angioid streaks, and thus with the degree of BM calcification. Possibly, the ICGA hypofluorescence in PXE patients is caused by impaired uptake of the indocyanine green (ICG) dye by the RPE as a result of decreased BM permeability. In a healthy eye, the indocyanine green dye diffuses outside the choroidal vessels and accumulates in the choroidal

interstitial tissue and RPE, which contributes to the fluorescence patterns in the late phase of ICGA.^{28–30} A less permeable BM resulting from calcification may inhibit the uptake of ICG dye by the RPE cells. This theory is supported by similar ICGA findings in patients with Sorsby dystrophy, also a disease with BM changes.³¹ Also, scattered ICGA hypofluorescence is associated with higher age in normal persons, and it correlates with soft drusen, which are local deposits of lipids in BM.^{32,33} Finally, the temporal island with reduced NIR correlates with an island of ICGA isofluorescence, which suggests that BM permeability is relatively normal in an area without BM calcification. We did not observe increased FAF in the areas with ICGA hypofluorescence, which reduces the probability of RPE dysfunction as the underlying mechanism of ICGA hypofluorescence in PXE. We hypothesize that ICGA hypofluorescence in PXE does not represent RPE dysfunction, but rather is the result of a reduced influx of ICG dye into the RPE cell because of a less permeable BM.

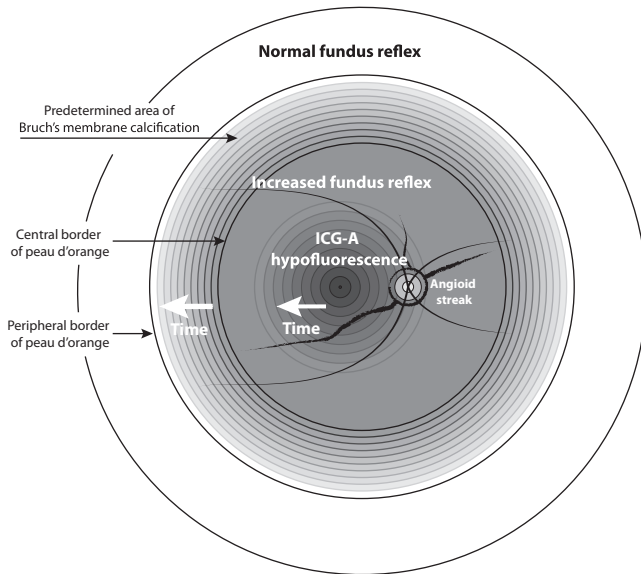


Figure 10. Diagram illustrating the proposed model for the changes in the fundus of a patient with pseudoxanthoma elasticum showing the changes that can be seen on different imaging methods. In the early disease stages, a predefined area for Bruch's membrane (BM) calcification already exists. This has a speckled aspect known as peau d'orange. This area will fill up with more confluent BM calcification over time that presents as an increased fundus reflex. Over time, a pattern of decreased indocyanine green angiography (ICGA) fluorescence appears that starts in the macula and spreads centrifugally. This model is a modification from the model as proposed by Charbel Issa et al.¹⁰

A surprising finding of this study was that the peripheral border of peau d'orange does not seem to be age dependent, but rather is a static feature of a PXE patient. During life, the area demarcated by the peripheral borders of peau d'orange fills up and the hyperreflective speckles confluence. Although a statistically significant association was found between the peripheral border and age in the cross-sectional analysis, the absolute difference between the youngest and oldest age groups was only 0.2 ODD. In the longitudinal analysis, we did not find a shift to the periphery; the equal distribution of positive and negative shifts in Figure 5A likely shows the variability of the measurement, rather than a true shift of the temporal border. Possibly, the sparse speckling at a young age has an impact on the visibility of the border. Therefore, we assume that the peripheral border, thus a predetermined area of BM calcification, is a static feature. The underlying pathologic characteristics of this predetermined area of BM calcification have yet to be unraveled. Possibly, PXE patients have a predisposition for calcification of a certain type of collagen or elastin fibers in BM or to a specific topographic area of BM. This is supported by the findings of Gheduzzi et al⁹ and Gorgels et al³⁴ that, apart from elastin fibers, collagen fibers also are affected, which was more pronounced in *ABCC6*^{-/-} mice than in humans. The predetermined area of BM calcification also may have other relevant structural characteristics, such as a thinner and more porous elastic layer.^{35,36} Chong et al³⁵ found that the elastic layer thickness increases rather abruptly at

14 to 16 mm temporal from the optic disc. This area correlates with the findings of our study: the median temporal border of peau d'orange was 15.4 mm (8.7 ODD, converted with a mean horizontal optic disc diameter of 1.77 mm).^{35,37} Furthermore, the 2 collagenous layers that enfold the elastic layer double in thickness in the peripheral region anterior to the equator, which corresponds with the location of histopathologic BM changes in PXE.^{38–40} Possibly, these topographic differences of the BM layers contribute to a predetermined area for calcification of fibers in BM. However, although it is plausible that the underlying topographic structure of BM and its properties play a role in the area of BM calcification in PXE, this remains speculative. A histopathologic correlation study with imaging is much needed to investigate the molecular and histopathologic changes underpinning PXE in the eye.

It is thought that angioid streaks are limited to the area with an increased fundus reflex in which BM changes are confluent and the BM is brittle and prone to break.^{10,14,41} Interestingly, we observed that in younger patients, angioid streaks often start in the area with an increased fundus reflex, but extend into the area of peau d'orange (Fig 2F). This finding suggests that the formation of angioid streaks does not depend only on confluent BM calcification.

Furthermore, we demonstrated that both angioid streaks and the central border of peau d'orange slowly progress during life, and younger patients show faster progression than older patients. Probably, the development of angioid streaks is an intermittent process, rather than a continuous process, because 75% of the angioid streaks did not change during follow-up, whereas cross-sectional analysis clearly showed progression during life. Factors such as mechanical stress or acute retinopathy may result in a sudden growth of angioid streaks.⁴² The reason why peau d'orange in younger patients seems to progress faster is unknown. Perhaps the shift in peau d'orange must be considered relative to the area with an increased fundus reflex because the confluence of a large concentric area of peau d'orange will take longer than the confluence of a smaller area. Moreover, variety exists among patients with regard to the age-specific extent of BM calcification: some patients progress faster than others (Fig 3B). Perhaps faster progression is associated with lower levels of inorganic pyrophosphate, an inhibitor of ectopic calcification implicated in the pathophysiologic characteristics of PXE.⁴³

We observed more macular angioid streaks with increasing age (Table 1), which was surprising to us because we observed little longitudinal changes of angioid streaks in the central 3000 μm in this study. The increasing prevalence may be explained by the slightly skewed gender distribution: our cohort included more men in the fifth decade of life than in the earlier decades. Possibly, women seek treatment earlier and more often with skin changes and mild fundus changes, whereas men more often seek treatment later with visual symptoms, around the fifth decade. Because these men seek treatment with visual symptoms, they likely have a higher prevalence of macular pathologic features resulting from

central angioid streaks. Based on our findings, angioid streaks in the central 3000 μm may progress, but do so very slowly, and the risk of growth during the course of a few years is very small.

Strengths of this study include the relatively large sample of PXE patients younger than 50 years, the use of follow-up data, and the use of different measurements based on multimodal imaging. A limitation of this study is that the longitudinal assessment of peau d'orange was not blinded for patients or for visits (baseline or follow-up). Theoretically, this may have led to an observer bias. However, we do believe that our measurements represent longitudinal progression because progression of peau d'orange is visible within an individual on longitudinal

imaging. Also, the cross-sectional age-specific data show a change at group level that suggests that individual progression must occur.

In summary, we described the natural course of different manifestations of BM calcification in PXE patients at an early disease stage. We hypothesize that a predetermined area for BM calcification exists that conflues with increasing age. The typical pattern of decreased indocyanine green fluorescence develops in the fourth or fifth decade and seems to depend on the extent of BM calcification. Histopathologic correlation with imaging is needed to explain the histopathologic processes accounting for the areas of peau d'orange, increased fundus reflex, and ICGA hypofluorescence.

Footnotes and Disclosures

Originally received: September 23, 2020.

Final revision: December 9, 2020.

Accepted: December 9, 2020.

Available online: December 19, 2020. Manuscript no. D-20-00007.

¹ Department of Ophthalmology, University Medical Center Utrecht, Utrecht University, The Netherlands.

² Department of Vascular Medicine, University Medical Center Utrecht, Utrecht University, The Netherlands.

Disclosure(s):

All authors have completed and submitted the ICMJE disclosures form.

The author(s) have no proprietary or commercial interest in any materials discussed in this article.

This study was supported by unrestricted grants from the Dr. F. P. Fischer Stichting; Rotterdamse Stichting Blindenbelangen; Stichting Vrienden UMC Utrecht; and Stichting PXE Fonds. The sponsors had no role in the design or conduct of this research.

HUMAN SUBJECTS: Human subjects were included in this study. The human ethics committees at University Medical Center Utrecht approved the study. All participants provided informed consent. All research adhered to the tenets of the Declaration of Helsinki.

No animal subjects were included in this study.

Author Contributions:

Conception and design: Risseeuw, van Leeuwen, Ossewaarde-van Norel
Analysis and interpretation: Risseeuw, van Leeuwen, Ossewaarde-van Norel

Data collection: Risseeuw, van Leeuwen, Ossewaarde-van Norel

Obtained funding: N/A

Overall responsibility: Risseeuw, van Leeuwen, Imhof, Spiering, Ossewaarde-van Norel

Abbreviations and Acronyms:

BM = Bruch's membrane; **CI** = confidence interval; **CNV** = choroidal neovascularization; **ICC** = intraclass correlation coefficient; **ICGA** = indocyanine green angiography; **IQR** = interquartile range; **NIR** = near-infrared reflectance; **ODD** = optic disc diameter; **PXE** = pseudoxanthoma elasticum; **RPE** = retinal pigment epithelium.

Keywords:

Bruch's membrane, Calcification, natural history, Peau d'orange, Pseudoxanthoma elasticum.

Correspondence:

Jeannette Ossewaarde-van Norel, MD, PhD, Department of Ophthalmology, University Medical Center Utrecht, Utrecht University, The Netherlands. E-mail: a.ossewaarde-vannorel@umcutrecht.nl.

References

- Bergen AAB, Plomp AS, Schuurman EJ, et al. Mutations in *ABCC6* cause pseudoxanthoma elasticum. *Nat Genet*. 2000;25:228–231.
- Plomp AS, Toonstra J, Bergen AAB, et al. Proposal for updating the pseudoxanthoma elasticum classification system and a review of the clinical findings. *Am J Med Genet A*. 2010;152A:1049–1058.
- Le Saux O, Urban Z, Tschuch C, et al. Mutations in a gene encoding an ABC transporter cause pseudoxanthoma elasticum. *Nat Genet*. 2000;25:223–227.
- Finger RP, Charbel Issa P, Ladewig MS, et al. Pseudoxanthoma elasticum: genetics, clinical manifestations and therapeutic approaches. *Surv Ophthalmol*. 2009;54:272–285.
- Risseeuw S, Ossewaarde-van Norel J, Klaver CCW, et al. Visual acuity in pseudoxanthoma elasticum. *Retina*. 2019;39:1580–1587.
- Gliem M, Muller PL, Birtel J, et al. Frequency, phenotypic characteristics and progression of atrophy associated with a diseased Bruch's membrane in pseudoxanthoma elasticum. *Invest Ophthalmol Vis Sci*. 2016;57:3323–3330.
- Gliem M, De Zaeytijd J, Finger RP, et al. An update on the ocular phenotype in patients with pseudoxanthoma elasticum. *Front Genet*. 2013;4:14.
- Jensen OA. Bruch's membrane in pseudoxanthoma elasticum. Histochemical, ultrastructural, and x-ray microanalytical study of the membrane and angioid streak areas. *Graefes Arch Clin Exp Ophthalmol*. 1977;203:311–320.
- Gheduzzi D, Sammarco R, Quaglini D, et al. Extracutaneous ultrastructural alterations in pseudoxanthoma elasticum. *Ultrastruct Pathol*. 2003;27:375–384.
- Charbel Issa P, Finger RP, Gotting C, et al. Centrifugal fundus abnormalities in pseudoxanthoma elasticum. *Ophthalmology*. 2010;117:1406–1414.

11. Charbel Issa P, Finger RP, Holz FG, Scholl HPN. Multimodal imaging including spectral domain OCT and confocal near infrared reflectance for characterization of outer retinal pathology in pseudoxanthoma elasticum. *Invest Ophthalmol Vis Sci.* 2009;50:5913.
12. Krill AE, Klien BA, Archer DB. Precursors of angioid streaks. *Am J Ophthalmol.* 1973;76:875–879.
13. Mansour AM, Ansari NH, Shields JA, et al. Evolution of angioid streaks. *Ophthalmologica.* 1993;207:57–61.
14. Jampol LM, Acheson R, Eagle RC, et al. Calcification of Bruch's membrane in angioid streaks with homozygous sickle cell disease. *Arch Ophthalmol.* 1987;105:93–98.
15. Kranenburg G, de Jong PA, Bartstra JW, et al. Etidronate for prevention of ectopic mineralization in patients with pseudoxanthoma elasticum. *J Am Coll Cardiol.* 2018;71:1117–1126.
16. Pomozi V, Julian CB, Zoll J, et al. Dietary pyrophosphate modulates calcification in a mouse model of pseudoxanthoma elasticum: implication for treatment of patients. *J Invest Dermatol.* 2019;139:1082–1088.
17. Risseeuw S, Ossewaarde-van Norel J, van Buchem C, et al. The extent of angioid streaks correlates with macular degeneration in pseudoxanthoma elasticum. *Am J Ophthalmol.* 2020;220:82–90.
18. Gliem M, Fimmers R, Müller PL, et al. Choroidal changes associated with Bruch membrane pathology in pseudoxanthoma elasticum. *Am J Ophthalmol.* 2014;158:644.
19. Risseeuw S, Bartstra J, Ossewaarde-van Norel J, et al. Is arterial stiffness in the carotid artery associated with choroidal thinning in patients with pseudoxanthoma elasticum or controls? *Acta Ophthalmol.* 2020. <https://doi.org/10.1111/aos.14346>. Online ahead of print.
20. Audo I, Vanakker OM, Smith A, et al. Pseudoxanthoma elasticum with generalized retinal dysfunction, a common finding? *Invest Ophthalmol Vis Sci.* 2007;48:4250–4256.
21. Hess K, Gliem M, Birtel J, et al. Impaired dark adaptation associated with a diseased Bruch membrane in pseudoxanthoma elasticum. *Retina.* 2020;40(10):1988–1995.
22. World Health Organization. ICD-10 definition. <http://apps.who.int/classifications/icd10/browse/2016/en>; 2016. Accessed 21.09.17.
23. Koo TK, Li MY. A guideline of selecting and reporting intraclass correlation coefficients for reliability research. *J Chiropr Med.* 2016;15:155–163.
24. Agarwal A, Patel P, Adkins T, Gass JDM. Spectrum of pattern dystrophy in pseudoxanthoma elasticum. *Arch Ophthalmol.* 2005;123:923–928.
25. Finger RP, Charbel Issa P, Ladewig M, et al. Fundus autofluorescence in pseudoxanthoma elasticum. *Retina.* 2009;29:1496–1505.
26. Gliem M, Hendig D, Finger RP, et al. Reticular pseudodrusen associated with a diseased bruch membrane in pseudoxanthoma elasticum. *JAMA Ophthalmol.* 2015;133:581–588.
27. Gliem M, Müller PL, Birtel J, et al. Quantitative fundus autofluorescence in pseudoxanthoma elasticum. *Invest Ophthalmol Vis Sci.* 2017;58:6159–6165.
28. Chang AA, Morse LS, Handa JT, et al. Histologic localization of indocyanine green dye in aging primate and human ocular tissues with clinical angiographic correlation. *Ophthalmology.* 1998;105:1060–1068.
29. Chang AA, Zhu M, Billson F. The interaction of indocyanine green with human retinal pigment epithelium. *Invest Ophthalmol Vis Sci.* 2005;46:1463.
30. Tam J, Liu J, Dubra A, Fariss R. In vivo imaging of the human retinal pigment epithelial mosaic using adaptive optics enhanced indocyanine green ophthalmoscopy. *Invest Ophthalmol Vis Sci.* 2016;57:4376–4384.
31. Gliem M, Müller PL, Mangold E, et al. Sorsby fundus dystrophy: novel mutations, novel phenotypic characteristics, and treatment outcomes. *Invest Ophthalmol Vis Sci.* 2015;56:2664–2676.
32. Chen L, Zhang X, Liu B, et al. Age-related scattered hypofluorescent spots on late-phase indocyanine green angiography: the multimodal imaging and relevant factors. *Clin Exp Ophthalmol.* 2018;46:908–915.
33. Chen L, Zhang X, Li M, et al. Drusen and age-related scattered hypofluorescent spots on late-phase indocyanine green angiography, a candidate correlate of lipid accumulation. *Invest Ophthalmol Vis Sci.* 2018;59:5237–5245.
34. Gorgels TGMF, Teeling P, Meeldijk JD, et al. Abcc6 deficiency in the mouse leads to calcification of collagen fibers in Bruch's membrane. *Exp Eye Res.* 2012;104:59–64.
35. Chong NHV, Keonin J, Luthert PJ, et al. Decreased thickness and integrity of the macular elastic layer of Bruch's membrane correspond to the distribution of lesions associated with age-related macular degeneration. *Am J Pathol.* 2005;166:241–251.
36. Hogan MJ, Alvarado J. Studies on the human macula: IV. Aging changes in Bruch's membrane. *Arch Ophthalmol.* 1967;77:410–420.
37. Quigley HA, Brown AE, Morrison JD, Drance SM. The size and shape of the optic disc in normal human eyes. *Arch Ophthalmol.* 1990;108:51.
38. Newsome DA, Huh W, Green WR. Bruch's membrane age-related changes vary by region. *Curr Eye Res.* 1987;6:1211–1221.
39. Klien BA. Angioid streaks. A clinical and histopathologic study. *Am J Ophthalmol.* 1947;30:955–968.
40. Verhoeff FH. Histological findings in a case of angioid streaks. *Br J Ophthalmol.* 1948;32:531–544.
41. Spaide RF. Peau d'orange and angioid streaks: manifestations of Bruch membrane pathology. *Retina.* 2015;35:392–397.
42. Gliem M, Birtel J, Müller PL, et al. Acute retinopathy in pseudoxanthoma elasticum. *JAMA Ophthalmol.* 2019;137(10):1165–1173.
43. Jansen RS, Kucukosmanoglu A, de Haas M, et al. ABCC6 prevents ectopic mineralization seen in pseudoxanthoma elasticum by inducing cellular nucleotide release. *Proc Natl Acad Sci U S A.* 2013;110:20206–20211.